EPR Investigation of the Active Site of Recombinant Human 5-Lipoxygenase: Inhibition by Selenide†

Tove Hammarberg,*,‡ Sergei Kuprin,§ Olof Rådmark, and Arne Holmgren

Department of Medical Biochemistry and Biophysics, Karolinska Institutet, Stockholm, Sweden

Received July 10, 2000; Revised Manuscript Received February 26, 2001

ABSTRACT: Lipoxygenases are a group of non-heme iron dioxygenases which catalyze the formation of lipid hydroperoxides from unsaturated fatty acids. 5-Lipoxygenase (5LO) is of particular interest for formation of leukotrienes and lipoxins, implicated in inflammatory processes. In this study, electron paramagnetic resonance (EPR) spectroscopy was used to investigate the active site iron of purified recombinant human 5-lipoxygenase (5LO), and to explore the action of selenide on 5LO. After oxidation by lipid hydroperoxides, 5LO exhibited axial EPR spectra typified by a signal at $g = 6.2$. However, removal of the lipid hydroperoxides, their metabolites, and the solvent ethanol from the samples resulted in a shift to more rhombic EPR spectra ($g = 5.17$ and $g = 9.0$). Thus, many features of 5LO and soybean lipoxygenase-1 EPR spectra were similar, indicating similar flexible iron ligand arrangements in these lipoxygenases. Selenide (1.5 μM) showed a strong inhibitory effect on the enzyme activity of 5LO. In EPR, selenide abolished the signal at $g = 6.2$, typical for enzymatically active 5LO. Lipid hydroperoxide added to selenide-treated 5LO could not reinstate the signal at $g = 6.2$, indicating an irreversible change of the coordination of the active site iron.

Lipoxygenases constitute a class of non-heme iron containing dioxygenases, which catalyze the incorporation of O_2 into 1,4-*cis*,*cis*-pentadiene-containing fatty acids. 5-Lipoxygenase (5LO)[1] catalyzes the two initial steps in the biosynthesis of leukotrienes from arachidonic acid: the stereospecific oxygenation leading to formation of (5S)-hydroperoxy-6-*trans*-8,11,14-*cis*-eicosatetraenoic acid (5-HPETE), and the further dehydration to leukotriene A_4. Leukotrienes play key roles in inflammatory reactions (*1*), especially in asthma where they are regarded as critical mediators; hence, 5LO is a drug target with considerable therapeutic potential. 5LO is mainly found in leukocytes, macrophages, and mast cells, and expression increases during differentiation and maturation of myeloid cells. The human enzyme is a monomeric 78 kDa protein that performs its catalysis at a lipid/water interface, and it is well established that 5LO enzyme activity is stimulated by Ca^{2+}, ATP, and phosphatidylcholine [for a review, see (*2*)].

In lipoxygenase catalysis, the active site iron is crucial for enzyme activity and switches between Fe^{2+} and Fe^{3+} during the catalytic cycle (*3*). So far, difficulties in producing large amounts of homogeneous enzyme for biophysical studies have hampered studies regarding the active site structure and catalytic mechanism of 5LO. Only one EPR study on 5LO has appeared (*4*). The well-studied and structure-determined lipoxygenase-1 from soybeans (SLO-1) has long served as a model protein regarding the catalytic mechanism and the nature of the iron center, for all lipoxygenases (*5*−*8*). This seems reasonable, since the highest degree of similarity between lipoxygenases is found around the amino acid residues that function as ligands to the active site iron (*9*). Furthermore, mutagenesis studies support an active site arrangement of 5LO similar to that of SLO-1 (*10*). More recently, crystal structures and spectroscopic studies on mammalian 15-lipoxygenases and on soybean lipoxygenase-3 have provided additional insights (*11*−*13*). The aim of the present study was to gain further information regarding the iron center in 5LO, by direct studies on purified recombinant enzyme using EPR.

Cellular 5LO activity is regulated by the peroxide tone. Phospholipid hydroperoxide glutathione peroxidase has been suggested to be primarily responsible for reduction of 5-HPETE in leukocytes (*14*). This peroxidase contains selenium, which is essential for activity. Thus, selenium and selenium compounds can inhibit 5LO indirectly, via selenium-dependent peroxidases, which suppress 5LO activity by reducing cellular lipid hydroperoxides needed to generate the activated ferric lipoxygenase. Interestingly, selenium compounds can also act as direct lipoxygenase inhibitors. The seleno-organic compound ebselen [2-phenyl-1,2-benzisoselenazol-3(2*H*)-one] has been shown to inhibit both 5LO

† This study was supported by grants from the Swedish Medical Research Council (03X-217 and 13X-3529), from the European Union, from the Verum Foundation, and (to S.K.) from Wenner−Grenska Samfundet and from Stiftelsen Ragnhild och Einar Lundströms Minne.

* Corresponding author. Telephone: + 46 8 162715. Fax: + 46 8 153679. E-mail: Tove.Hammarberg@dbb.su.se.

‡ Present address: Department of Biochemistry and Biophysics, Arrhenius Laboratory, Stockholm University, SE-106 91 Stockholm.

§ Present address: Plasma Products, P19:1, Pharmacia Corp., SE-11287 Stockholm, Sweden.

[1] Abbreviations: 5LO, mammalian 5-lipoxygenase (EC 1.13.11.34); SLO-1, soybean lipoxygenase-1; 5-HPETE, 5(*S*)-hydroperoxy-(6*E*; 8, 11, 14*Z*)-eicosatetraenoic acid; 15-HPETE, 15(*S*)-hydroperoxy-(5, 8, 11*Z*; 13*E*)-eicosatetraenoic acid; 13-HPOD, 13(*S*)-hydroperoxy-(9*Z*; 11*E*)-octadecadienoic acid; EPR, electron paramagnetic resonance; *g*, electron *g* factor; *D* and *E*, axial and rhombic zero-field splitting constants; ***B***, magnetic flux.

10.1021/bi001595d CCC: $20.00
Published on Web 05/03/2001

and 15LO in the absence of glutathione (*15*, *16*). Selenite and seleno-diglutathione (GS-Se-SG) have been shown to efficiently inhibit 5LO activity in human B-lymphocytes (*17*). After reduction by, e.g., the thioredoxin system, these compounds were suggested to yield selenide, which may interact directly with the 5LO active site iron. This proposal was supported by EPR studies on SLO-1, in which chemically generated selenide was shown to reduce the iron in oxidized enzyme (*17*). In analogy, ebselen was recently reported to alter the geometry of the iron ligand sphere in mammalian 15LO (*18*).

In this paper, results from EPR studies on the iron center of 5LO are reported. The effect of ethanol and lipid hydroperoxide on the ferric iron center is described. We also show that selenide is a potent inhibitor of purified 5LO, and a direct interaction between chemically generated selenide and the active site iron of 5LO is demonstrated.

EXPERIMENTAL PROCEDURES

Materials. Selenite, sodium borohydride, and DMSO were from Sigma. 15-HPETE was a kind gift from Professor Mats Hamberg, Karolinska Institute. 5-HPETE and 13-HPOD (purified by normal-phase HPLC) were from Biomol (Plymouth Meeting, PA). We routinely confirmed the identity and concentration of these lipid hydroperoxides by analytical reverse-phase HPLC and UV spectroscopy. Elemental selenium was kindly provided by Dr. Göran Zdansky, Uppsala University, Sweden, and the Fe^{3+}-EDTA standard was a kind gift from Dr. Peter Schmidt, Stockholm University, Sweden. Other chemicals were from Merck (Germany).

5LO Protein Preparation and Analyses. Recombinant human 5LO was expressed in *E. coli* and purified to >95% purity according to previously described methods (*19*−*21*). The purified enzyme (0.2−10 mg/mL) was kept in the ATP elution buffer in the presence of the stabilizing enzymes, glutathione peroxidase and superoxide dismutase (*16*), at −70 °C until the day of the experiment.

5LO protein concentration was estimated as described by Bradford (*22*), using a protein assay kit from Bio-Rad with bovine serum albumin as standard. A molecular mass of 78 kDa was used in the calculations.

Optical and UV absorption spectra were recorded using a PC-interfaced Shimazu 2000 spectrophotometer.

Preparation of Selenide. Selenide was prepared by reduction of elemental selenium exactly as described in (*17*). Dilutions of the stock solution of selenide were made anaerobically with 50 mM Tris-HCl, pH 7.5, which had been flushed with argon. Pure argon (AGA, Sweden) was used to purge solutions from oxygen. Argon was additionally purified from oxygen and saturated by H_2O by the passage through a fresh 0.2% solution of $Na_2S_2O_4$ in 0.1 M NaOH.

5LO Cuvette Activity Assay. 5LO (70 μg/mL) was preincubated at room temperature for 30−60 min anaerobically or in air-saturated buffer (50 mM Tris-HCl, pH 7.0) containing selenide (1.5 μM). Control samples were made without selenide. In a cuvette, 100 μL of the preincubate was added to 900 μL of substrate solution (50 mM Tris, pH 7.5, 0.2 mM ATP, 30 μM EDTA, 0.1 mM $CaCl_2$, 20 g/mL phosphatidylcholine, 1 mM DTT, 75 μM arachidonic acid with or without 2.5 μM 13-HPOD). The production of 5-HPETE was followed by monitoring the absorbance at 234 nm.

Preparation of EPR Samples. The active site iron of 5LO was oxidized by incubating 5LO protein samples (50−150 μM) with 1−5 molar equiv of lipid hydroperoxide (5-HPETE, 15-HPETE, or 13-HPOD dissolved in ethanol or DMSO) at room temperature for 2−5 min. Low molecular weight components, including the hydroperoxides and their products, were removed from the samples by a single passage through a Sephadex G25 centrifuge column, equilibrated with 50 mM Tris-HCl, pH 7.2, as described previously (*17*). About 200 μL of each sample was transferred into EPR tubes under a flow of argon. Control samples were prepared without enzyme.

Samples assigned to selenide treatment were handled under a flow of argon, anaerobic buffers (see "Preparation of Selenide") were used, and all tubes were prerinsed with oxygen-free buffers and purged from oxygen by blowing argon on the surface for 40 min.

EPR Measurement. X-band EPR spectra were recorded on a Bruker 300 spectrometer as in (*17*, *23*) at 3.6−21 K, equipped with a pumped helium flow cryostat EPR-9 from Oxford Instruments. Samples were measured in a dual mode cavity (Bruker ER4116 DM), which easily allowed switching between the normal perpendicular to the main field orientation of the microwave field, $\mathbf{B}_1 \perp \mathbf{B}$, and the parallel mode, $\mathbf{B}_1 \| \mathbf{B}$, by a slight ∼300 MHz decrease of the spectrometer frequency. The microwave frequency was measured prior to each scan with a Hewlett-Packard 5350A microwave frequency meter. The modulation frequency was 100 kHz. Only linear baseline corrections were applied.

Intensities of components were estimated from double integrals of EPR spectra and referred to the intensities of the Fe^{3+}-EDTA standard sample measured at the same temperature as the sample of interest. Relative intensities of axial components, observed at $g \sim 6.1$, were measured also as ratios of magnitudes of the corresponding peaks in the absorption derivative spectra (*24*). Power saturation data were collected by measuring the EPR absorption derivative peak signal intensity as a function of incident microwave power (P). In the case of $g = 4.28$ signals, peak-to-peak intensities (I) of the sharpest component were measured. The half-saturation power values, $P_{1/2}$, were determined graphically by plotting $(I/P^{0.5})/(I/P^{0.5})_{max}$ versus $\log(P)$. $P_{1/2}$ values are defined as abscissas of the points of crossings of linear interpolations of the dependencies at high powers with the level 0.707 (*25*).

EPR spectra of Fe^{3+} ions were analyzed in the framework of Spin-Hamiltonian formalism (*26*), using the standard Spin-Hamiltonian for the $S = 5/2$ spin system (*27*):

$$\boldsymbol{H} = g\beta\boldsymbol{BS} + D[\boldsymbol{S}_z^2 - \boldsymbol{S}(S+1)/3] + E[\boldsymbol{S}_x^2 - \boldsymbol{S}_y^2] \quad (1)$$

Here g is the electron g factor, β is the Bohr magneton, D and E are the axial and rhombic zero-field splitting constants, respectively, $\boldsymbol{B}$ is the applied magnetic field, and $\boldsymbol{S}_i$ ($i = x, y, z$) are the operators for electron spin angular momentum.

Temperature dependencies of EPR signals were approximated by the equation (*28*, *29*):

$$N = T^{-1}AN_0[1 + \exp(-2D/kT) + \exp(-6D/kT)]^{-1} \quad (2)$$

where k is the Boltzmann constant, N is the signal intensity, N_0 was the fitted parameter, and $A = 1$ for the ground-state

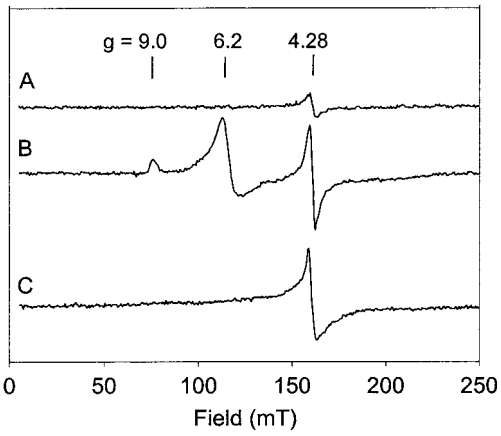

FIGURE 1: EPR spectra of human 5-lipoxygenase: native and oxidized with 15-HPETE. (A) Native 5LO (20 nmol) in 200 μL of ATP purification buffer (50 mM triethanolamine, pH 7.3, 100 mM NaCl, 12 mM ATP, 15 mM 2-mercaptoethanol) containing 2 mM CHAPS. (B) Sample A was thawed and incubated with 47 nmol of 15(*S*)-HPETE in ethanol (final content 1.5 vol %) at room temperature for 5 min. (C) Fe^{3+} standard, 360 μM. Instrumental parameters: microwave power, 10 mW; modulation amplitude, 1.1 mT; temperature, 3.7 K; microwave frequency, 9.617 GHz, at normal, perpendicular mode ($\mathbf{B}_1 \perp \mathbf{B}$).

transitions and $A = \exp(-2D/kT)$ for the $g \sim 4.3$ and $g \sim 5.2$ lines of the transitions of excited states.

Spectral manipulations, integration, Fourier transformations, etc. were made with the help of the spectrometer software and also with the help of the program Octave running on a PC under a Linux operating system. The fitting and plotting was done with the help of the program GraFit (*30*).

RESULTS

EPR Investigations of the Iron Center in 5LO. EPR spectra of native and oxidized 5LO are shown in Figure 1. The native sample of 5LO was EPR-silent, apart from the signal at $g = 4.28$ (trace A), which coincided with the signal from ionic Fe^{3+} (trace C). We assigned the $g = 4.28$ peak in the native 5LO sample to adventitiously bound iron. After oxidation with lipid hydroperoxide [2.4 molar equiv of 15(*S*)-HPETE in ethanol], a major peak at $g = 6.2$ appeared (trace B), in accordance with an axial type EPR signal from ferric 5LO. This was observed also in the previous EPR study on 5LO (*4*). The increased signal at $g = 4.28$ may be derived from iron, which had been released from degraded 5LO, or from a rhombic iron center in inactivated 5LO. The signal of low intensity at $g = 9.0$ is discussed below.

We performed microwave power saturation studies at 3.6 K and determined $P_{1/2} = 7.4$ mW for the $g = 6.2$ signal and $P_{1/2} = 3$ mW for the $g = 4.28$ signal. The temperature dependence of the signal intensity measured at 10 mW was in agreement with the Spin-Hamiltonian model for the $S = 5/2$ spin system with a positive D value (eq 1), which predicts that the $g = 6.2$ signal would decrease with the increase of observation temperature. Fitting of the temperature dependence data with eq 2 gave the zero-field splitting constant, $D \cong 2$ cm^{-1}.

We found that either the oxidizing lipid hydroperoxides, their alcohol products, or ethanol was needed to be present in the 5LO samples for a prominent $g = 6.2$ signal to be obtained. This is illustrated in Figure 2. In this experiment,

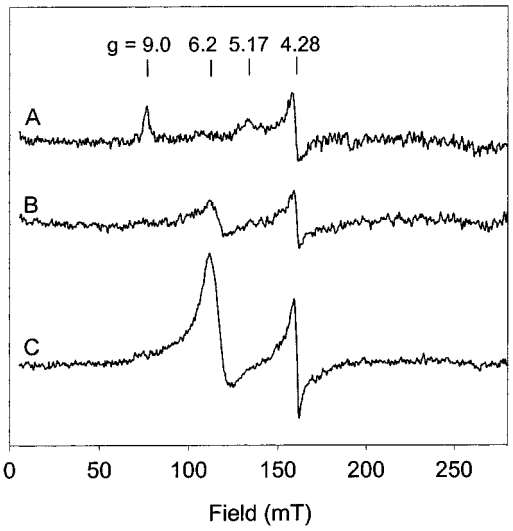

FIGURE 2: Effects of ethanol on the EPR spectra of human 5-lipoxygenase oxidized with 5-HPETE. (A) 5LO (14 nmol, in 200 μL of ATP purification buffer: 50 mM triethanolamine, pH 7.3, 100 mM NaCl, 12 mM ATP, 15 mM 2-mercaptoethanol) was incubated with 5(*S*)-HPETE (25 nmol) in ethanol (2 vol %) for 2 min at room temperature and subsequently gel-filtered into deaerated 50 mM Tris buffer, pH 7.2, using a Sephadex G25 spin column. (B) Sample A was thawed, and 2 vol % of ethanol was added. (C) Sample B was thawed and 5(*S*)-HPETE (25 nmol) was added, the sample was incubated for 2 min at room temperature, and the final ethanol concentration became 4.8 vol %. Instrumental parameters: temperature, 3.6 K; microwave power, 100 mW; microwave frequency, 9.617 GHz; modulation amplitude, 1.1 mT at normal, perpendicular mode ($\mathbf{B}_1 \perp \mathbf{B}$).

5LO was oxidized by incubation with 5-HPETE. Before the EPR determination, excess 5-HPETE, 5-HETE, and the solvent ethanol were removed from the sample by spin column gel filtration (trace A). Together with a faintly visible axial signal at $g = 6.2$ and the rhombic component at $g = 4.28$, we observed two additional signals: one at $g = 9.0$ and another at $g = 5.17$. The intensity of the former signal was decreasing, while that of the latter signal was increasing with observation temperature, suggesting that these signals represent different transitions of the same Fe^{3+} center. Comparison of the line positions with $g = f(E/D)$ rhombograms for the $S = 5/2$ spin system (*27*) allowed us to assign the described signals to an Fe^{3+} center of moderate rhombicity: $E/D \approx 0.2$. The $g = 9.0$ signal would arise from the ground-state transitions and the $g = 5.17$ signal from the excited-state transitions. In the temperature interval of 3.5−10 K, it was not possible to saturate these signals by a microwave power of up to 100 mW. Such behavior indicates a smaller value of the zero-field splitting constant, D, for this center as compared to the $D = 2$ cm^{-1} value for the $g = 6.2$ center. Signals at $g = 9.0$ and $g = 5.17$ can be seen also in Figure 1, trace B; Figure 3, traces B and C; and Figure 6, trace A.

The moderately rhombic iron center in Figure 2, trace A, could be converted into a center close to the axial limit, $E/D \rightarrow 0$, by the addition of alcohol. This is shown in Figure 2, trace B, where the addition of ethanol (2% v/v) led to the disappearance of the signals at $g = 9.0$ and $g = 5.17$, and simultaneously to the appearance of the axial $g = 6.2$ signal. Further addition of 5-HPETE resulted in a more pronounced axial signal (Figure 2, trace C), showing that the iron in the trace B sample was not fully oxidized. Also the intensity of

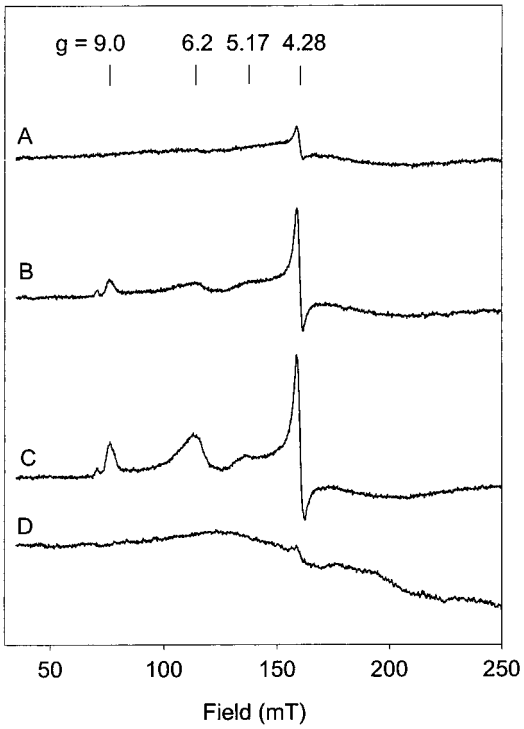

FIGURE 3: EPR spectra of human 5-lipoxygenase: native and oxidized with 13-HPOD. (A) Native 5LO (21 nmol) in 150 μL of ATP purification buffer (50 mM triethanolamine, pH 7.3, 100 mM NaCl, 12 mM ATP, 15 mM 2-mercaptoethanol). (B and C) Aliquots of sample A were incubated at room temperature for 3 min with 21 nmol of 13(*S*)-HPOD in EtOH (1.7 vol %) and 42 nmol of 13-(*S*)-HPOD in EtOH (3.4 vol %), respectively. (D) ATP purification buffer (see above). Instrumental parameters: temperature, 4.1 K; microwave power, 100 mW; microwave frequency, 9.620 GHz; modulation amplitude, 1.1 mT at normal, perpendicular mode ($\mathbf{B}_1 \perp \mathbf{B}$).

the signal at $g = 4.28$ increased. This is most likely due to oxidation of adventitiously bound iron, which was not separated by the quick pass through the Sephadex spin column, but we could not exclude that this signal represents a population of 5LO possessing an iron center with a rhombic symmetry. We considered the possibility that excess lipid hydroperoxide could result in a purple form of 5LO, as in the case of SLO-1. However, no such species was observed in optical spectra of 5LO recorded in the presence of any of the lipid hydroperoxides used in this study (data not shown).

To achieve complete oxidation of the active site iron in our samples, addition of lipid hydroperoxide in molar excess over protein was required (Figure 3). This was seen not only for the tetraenoic compounds 5-HPETE and 15-HPETE (Figures 1, 2, and 4), but also when the dienoic 13-HPOD was used as oxidant (Figure 3). One reason for the requirement of excess lipid hydroperoxide may be the presence of 2-mercaptoethanol (15 mM) in our enzyme samples. In control experiments, we found that one-third of lipid hydroperoxide (160 nM) added to ATP elution buffer containing 2-mercaptoethanol (15 mM) was reduced to the corresponding hydroxide within 3 min at room temperature. One may also speculate that other entities on 5LO (other than the iron) could be subject to oxidation, consuming lipid hydroperoxide.

In contrast to ethanol, DMSO (up to 3% v/v, data not shown) did not affect the EPR spectrum of 5LO. However, the presence of ethanol was not required for the axial signal to appear; addition of lipid hydroperoxide dissolved in

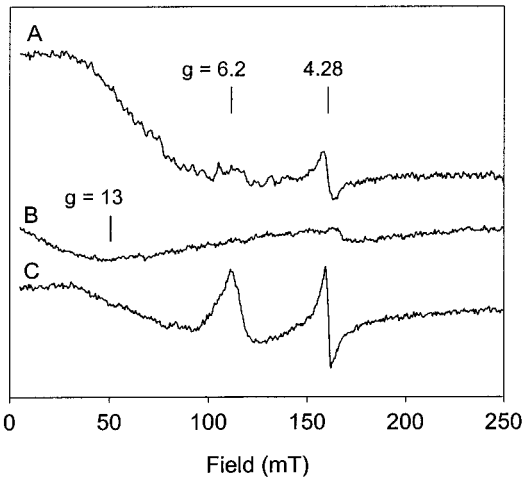

FIGURE 4: EPR spectra of human 5-lipoxygenase oxidized with lipid hydroperoxides dissolved in DMSO. (A) 5LO (15 nmol) in 200 μL of ATP purification buffer (50 mM triethanolamine, pH 7.3, 100 mM NaCl, 12 mM ATP, 15 mM 2-mercaptoethanol) was incubated at room temperature for 5 min with 42 nmol of 15(*S*)-HPETE in DMSO (2.5 vol %), subsequently gel-filtered into 50 mM Tris buffer, pH 7.2, using a Sephadex G25 spin column, and recorded at normal, perpendicular mode ($\mathbf{B}_1 \perp \mathbf{B}$) and (B) at parallel mode ($\mathbf{B}_1 \parallel \mathbf{B}$). (C) The sample was thawed, incubated with 30 nmol of 5(*S*)-HPETE in DMSO (final content 3.3%) at room temperature for 5 min, frozen, and recorded at normal mode. Instrumental parameters: microwave power, 100 mW; modulation amplitude, 1.1 mT; temperature, 3.6 K; microwave frequency, 9.617 GHz for (A) and (C), 9.336 GHz for (B).

DMSO also gave a pronounced signal at $g = 6.2$ (Figure 4). The broad feature at $\boldsymbol{B} < 100$ mT, which is present in the spectrum from partially oxidized 5LO (trace A), may tentatively be ascribed to ferrous 5LO, as suggested by Chasteen et al. (*4*), but could also have other origins. The spectrum in trace B in Figure 2 was recorded under the condition of $\mathbf{B}_1$ parallel to $\mathbf{B}$. As in the case of other metal complexes with an integer value of the total spin (*31*, *32*), this spectrum revealed a broad trough-looking feature at low magnetic field with a minimum approximately at $g = 13$.

Calcium, ATP, and phosphatidylcholine are known to stimulate the catalytic activity of 5LO in vitro. However, no significant changes in the spectrum of a completely oxidized 5LO in the presence of ethanol (like trace C in Figure 2) were detected after addition of $CaCl_2$ (0.5 mM), ATP (0.8 mM), and phosphatidylcholine (120 μg/mL) (data not shown). In experiments where preoxidized 5LO (0.16 mM) was incubated for 5 min with the substrate arachidonic acid (2 mM), we were not able to detect the axial $g = 6.2$ signal of the ferric iron center. Only an intense $g = 4.28$ signal was detected (data not shown). This was accompanied by a complete loss of enzyme activity (activity assays of thawed EPR samples). Loss of activity was also observed upon thawing, followed by a prolonged (more than 20 min) aerobic incubation at room temperature, of 5LO samples which had been oxidized by 5-HPETE, or 15-HPETE or 13-HPOD. Thus, turnover and/or aeration led to destruction of the iron center, compatible with loss of activity. We relate the ability of 5LO to exhibit the axial EPR signal to enzymatically active protein. Spectra with solely rhombic signals were recorded from less active or inactive samples. Also, preliminary EPR spectra of mutated 5LO proteins, which were enzymatically inactive (mutations of H367), gave only rhombic signals in EPR (not shown).

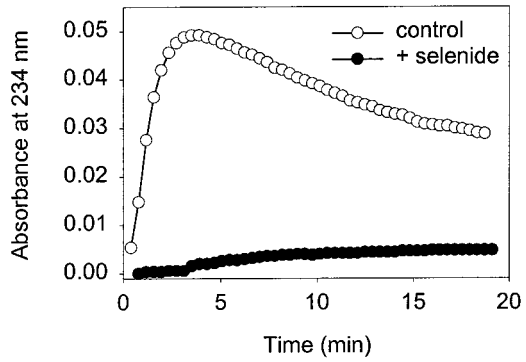

FIGURE 5: Inhibition of 5LO activity by selenide. 5LO (130 nM) was preincubated in deaerated 50 mM Tris-HCl, pH 7.2, in the absence (open circles) or in the presence (filled circles) of 1.5 μM selenide for 1 h at room temperature. The preincubate was diluted 10-fold into 50 mM Tris-HCl, pH 7.5, 0.2 mM ATP, 0.1 mM $CaCl_2$, 30 μM EDTA, 0.075 mM arachidonic acid (AA), 20 μg/mL phosphatidylcholine (PC), 1 mM DTT. The absorbance at 234 nm was recorded every 20 s, for 19 min.

Effects of Selenide on 5LO Activity and on the Iron Center of 5LO. Incubation of purified recombinant 5LO (130 nM) with 1.5 μM chemically generated selenide in argon-purged (deaerated) buffer resulted in loss of enzyme activity (Figure 5). Similar inhibition by selenide was observed when the enzyme catalysis activator, 13-HPOD (2.5 μM), was present in the 5LO activity assay (data not shown). Selenide is not stable under aerobic conditions and showed no inhibitory effect when the preincubation was performed in aerobic buffer. The extent of inhibition, measured as a percentage of a maximal velocity relative to the control sample, increased with time of preincubation with selenide. At 1.5 μM selenide, ~60% of the control activity remained after 10 min, ~40% after 20 min, and ~5% after 1 h. Thus, an apparent second-order rate constant for the reaction could be estimated to be approximately 500 M^{-1} s^{-1}. The inhibition increased drastically at higher concentration of selenide (data not shown).

We next determined the putative direct interaction between selenide and the active site in 5LO by EPR. A sample of 5LO was first oxidized by treatment with 15-HPETE (3 equiv), and then gel-filtered under anaerobic conditions to remove oxygen and excess lipid hydroperoxide. EPR resulted in trace A in Figure 6, with features at $g = 9$, $g = 6.2$, $g = 5.13$, and $g = 4.28$. These features were not seen in the spectrum of trace B, in which another aliquot of the same sample was supplied also with selenide prior to measurement by EPR. Neither did addition of more lipid hydroperoxide (5-HPETE, 2 equiv) to sample B generate the EPR signals (see trace C). Additional thawing of this sample and aeration at room temperature for 5 min resulted in the appearance of signals at $g = 9.8$ and $g = 4.28$, attributed to an Fe^{3+} center of high rhombicity, $E/D \rightarrow 0.33$, or to non-enzyme-bound Fe^{3+} (trace D). At the end of the experiment, the 5LO in this selenium-containing sample was completely inactive. When another aliquot of the sample giving EPR spectrum A was treated with 5-HPETE (2 equiv in DMSO) in the absence of selenide, the expected intense signal at $g = 6.2$ was obtained (trace E). This sample was thawed, selenide was added, and a second spectrum was recorded (trace F). Again, we obtained a complete loss of the axial signal at $g = 6.2$, but the $g = 4.28$ component was unaffected. The selenide concentration used in the EPR samples was much higher (3 mM) than the inhibitory concentration in the activity assay (1.5 μM). This was due to the high protein concentration demanded in EPR spectroscopy. The 5LO: selenide ratio, however, was in the same range in the two types of experiments.

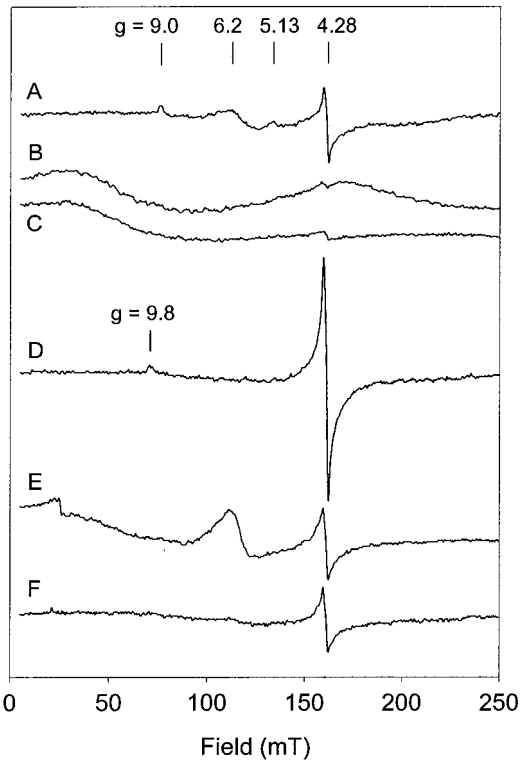

FIGURE 6: EPR spectra of oxidized 5LO treated with selenide. (A) 5LO (15 nmol) in 200 μL of ATP purification buffer (50 mM triethanolamine, pH 7.3, 100 mM NaCl, 12 mM ATP, 15 mM 2-mercaptoethanol) was incubated at room temperature for 5 min with 42 nmol of 15(*S*)-HPETE in DMSO (2.5 vol %), subsequently gel-filtered into deaerated 50 mM Tris buffer, pH 7.2, using a Sephadex G25 spin column, transferred into an anaerobically treated EPR tube, and frozen. (B) A sample parallel to that in (A) was supplied with selenide (600 nmol) before transfer to the EPR tube. (C) Sample B was thawed and incubated for 3 min at room temperature with extra 5(*S*)-HPETE (30 nmol) (DMSO content became 3.3%). (D) Sample C was thawed, aerated, and incubated for 5 min at room temperature. (E) A sample parallel to that in (A), except that this sample was gel-filtered and manipulated under aerobic conditions, was incubated for 3 min at room temperature with extra 5(*S*)-HPETE (30 nmol) (DMSO content became 3.3%). (F) Sample E was thawed and incubated for 3 min at room temperature with 300 nmol of selenide. Instrumental parameters: microwave power, 100 mW; modulation amplitude, 1.1 mT; temperature, 3.6 K; microwave frequency, 9.617 GHz, at normal perpendicular mode ($\mathbf{B}_1 \perp \mathbf{B}$).

In summary, it appeared that ferric iron in oxidized 5LO was reduced by selenide. However, it seems clear that selenide did not only cause a simple reduction of the iron. Instead an irreversible modification occurred which prevented reoxidation by lipid hydroperoxide. After aeration of a selenide-treated sample, only the rhombic component at $g = 4.28$ increased, which may represent ferric iron in a destroyed iron center, or iron ions which had been released from damaged 5LO. Oxidation by O_2 did not restore the $g = 6.2$ signal, characteristic for enzymatically active 5LO.

DISCUSSION

The oxidized form of the active site iron in recombinant human 5LO (expressed in *E. coli*) gave an axial EPR

Table 1: Ligands to the Active Site Iron in Four Lipoxygenases[a]

enzyme	ligand 1	ligand 2	ligand 3	ligand 4	ligand 5	ligand 6
SLO-1	H499	H504	H690	N694	C-term I839	H_2O
SLO-3	H518	H523	H709	N713	C-term I857	
rabbit 15LO	H361	H366	H541	H545	C-term I663	
5LO	H367	H372	H550	N554	C-term I673	

[a] Data for the enzymes in rows 1−3 originate from their solved crystal structures (*7*, *11*, *12*). Regarding 5LO, the ligands find support in sequence alignments, mutagenesis studies, and EPR data of the present study.

spectrum (Figures 1−4). This is in agreement with the previous report on Fe^{3+} EPR spectra of recombinant human 5LO (expressed in *Sf* cells) (*4*). However, one difference was our consistent requirement of excess lipid hydroperoxide (about 2 equiv) in order to get clear Fe^{3+} signals, while Chasteen reported that 1 equiv was sufficient (*4*). This discrepancy may be due to the presence of 2-mercaptoethanol in our 5LO samples. We also found that the presence of alcohol influenced the iron ligand sphere of 5LO, as previously described for soybean lipoxygenase-1 (SLO-1) (*33*−*38*). New signals, of moderate rhombicity, became more intense relative to the $g = 6.2$ signal when the lipid hydroperoxide oxidant, its products, and the solvent ethanol were removed from the sample by gel filtration after incubation (Figure 2). These moderately rhombic signals ($g = 9.0$ and $g = 5.17$) were replaced by the axial signal at $g = 6.2$ upon re-addition of ethanol or lipid hydroperoxide to a gel-filtered oxidized 5LO sample. This indicates a flexibility of the iron center in 5LO.

Studies on SLO-1 and mammalian 15LOs have led to the conclusion that axial EPR spectra originate from Fe^{3+} species which contain four equally strong ligands in one plane and a perpendicular axis defined by two ligands of which one deviates in binding strength (much weaker or stronger) compared to the other ligands (*13*, *39*). The axial EPR spectrum obtained for ferric 5LO in the presence of ethanol and/or lipid hydroperoxide, which is similar to EPR results for SLO-1, is in agreement with such a ligand arrangement. The observed positive *D*-value would suggest the off-plane ligand to be weak (*13*), which would fit with an asparagine residue (N554) as ligand 4 in 5LO (Table 1), analogous to N694 in SLO-1. The moderately rhombic EPR spectrum of ferric 5LO, obtained after removal of ethanol/lipid hydroperoxide, indicates a structure more close to an iron center with six equally strong ligands. This may arise when a weak endogenous ligand binds stronger or is substituted by a stronger exogenous ligand. The switch from a moderately rhombic to an axial EPR spectrum, observed when the oxidant and alcohol were added, suggests that ethanol, lipid hydroperoxide, or a metabolite may influence the geometry of iron coordination.

Flexibility of the iron coordination in lipoxygenases has been suggested to play a critical role in regulation of enzyme activity (*13*, *39*−*41*). For SLO-1 and human 15LO, ligand 4 (Table 1) and its interaction with the iron have been suggested to tune the catalytic reactivity (*40*). The status of N694 in SLO-1 as a relatively weak ligand was correlated to the high reduction potential of the active site iron, which has been reported for SLO-1 (*42*). Possibly also in this respect parallels could be drawn between 5LO and SLO-1, meaning that the status of N554 as a flexible ligand to the iron in 5LO would lead to high catalytic efficiency by destabilizing the ferric state.

Comparison of crystallographic data has shown that the mononuclear non-heme iron sites of lipoxygenases are related to active sites of other enzyme families, characterized by a common structural motif, referred to as the 2-His-1-carboxylate facial triad (*43*). Based on sequence comparisons with the structure-determined lipoxygenases (Table 1), the ligands that would form this triad in 5LO are the following: two nitrogens of H372 and H550 and one of the carboxylate oxygens of the C-terminal I673. Unlike other 2-His-1-carboxylate facial triad enzymes, lipoxygenases contain two additional endogeneous ligands to the iron: N554 and H367 in the case of 5LO. This is consistent with our previously suggested subdivision of the putative iron ligands of 5LO into permanent (H372, H550, I673) and flexible or replaceable (H367, N554) ligands, based on mutagenesis data (*20*, *44*, *45*). By temporary breaking (or weakening) the bond to the iron, a flexible ligand would make it possible for other atoms of, e.g., the substrate to interact with the enzyme. This property may be of relevance in the reaction mechanism of 5LO. The lipoxygenation reaction is significantly different from the catalytic mechanism of many other enzymes with the 2-His-1-carboxylate triad motif, in the sense that the ferrous active site does not react with O_2 (*46*). Instead the ferric lipoxygenase iron is believed to be involved in the activation of the substrate (by hydrogen abstraction). A change in the iron coordination, coupled to a close contact between the iron and a carbon at the position of the 1,4-diene unit of the substrate, may be of importance for such activation (*47*). In the refined crystal structure of SLO-1 (1.4 Å resolution), a water molecule is identified as a sixth iron ligand in native ferrous SLO-1 (see Table 1) (*7*). Also the iron centers of mammalian 15LOs and SLO-3 are expected to contain a water ligand (*12*, *38*, *39*, *48*). It was suggested that this water molecule could be substituted by an organic substrate (*39*).

Although 5LO shares many spectroscopic properties with SLO-1, there are also signs of differences in their iron centers. In the presence of 13-HPOD in molar excess to the enzyme, solutions of SLO-1 turn purple (*49*, *50*). This purple form of SLO-1 protein is thought to consist of enzyme-bound intermediates formed during oxygenation of linoleic acid (*51*). The EPR spectrum of purple ferric SLO-1 is rhombic, and the conversion from the axial to the rhombic EPR spectrum has been suggested to reflect a reversible replacement of the water ligand by the lipid hydroperoxide (*39*). No purple form of 5LO is known, and in accordance, the EPR spectrum did not change upon addition of 5-HPETE or 13-HPOD in excess (up to 5 equiv) [the present study and ref (*4*)]. Instead, the presence of lipid hydroperoxide seemed to favor and stabilize the axial state of 5LO.

Ca^{2+}, ATP, and phosphatidylcholine are well-known activators of 5LO activity in vitro. Recently, we described that both Ca^{2+} and ATP bind independently and specifically to the enzyme (*21*, *52*, *53*). When these activators were added to 5LO samples, there were no significant effects on EPR spectra. The lack of effect on the iron center of the enzyme indicates that the binding sites for these regulatory cofactors may be distant from the active site, which is in accordance with the recently proposed binding regions (*21*, *53*).

The previously suggested direct inhibitory effect of selenide on 5LO (*17*) was confirmed for purified enzyme in the present study. Furthermore, EPR experiments showed that selenide caused irreversible changes of the iron center in 5LO. The axial EPR signal, characteristic for active enzyme, disappeared upon the addition of selenide. After subsequent destruction (oxidation) of the selenide by exposure to air, we were not able to recover the axial signal. Selenide may react with protein −SH groups, and thereby inhibit enzyme activity by introducing conformational changes. However, such interactions alone would not explain the reduction of the active site iron. It appears possible that selenide substitutes for, or reacts with, a natural iron ligand in 5LO, thereby preventing enzyme catalysis. A similar mechanism was recently suggested for the inhibition of mammalian 15LO by ebselen (*18*). Since selenide was not inhibitory when added to 5LO in the presence of oxygen, a reactive oxygen species (formed by reaction between selenide and oxygen) should not be the inhibitory species. We found a profound inactivation of 5LO at selenide concentrations as low as 1.5 μM. One may expect that in tissues, selenide could easily be produced in such amounts from selenodiglutathione or from externally added selenium compounds with the help of cellular thioredoxin and/or glutaredoxin systems (*54*, *55*).

By direct interaction with the active site iron, several selenium-containing compounds and their cellular metabolites may inhibit 5LO. For instance, ebselen is a direct substrate for mammalian thioredoxin reductase (*56*), giving rise to the highly reactive ebselen selenol, which should inhibit 5LO. Also naturally occurring cellular selenium-containing compounds might influence 5LO. Mammalian thioredoxin reductase itself, which has a broad substrate specificity and has been shown to reduce lipid hydroperoxides (*57*), contains an essential seleno-cysteine residue in an open active site (*58*). Possibly, this enzyme can react directly with 5LO. In general, selenium compounds equipped with structural features making them 5LO selective could be considered as potential 5LO inhibitors.

ACKNOWLEDGMENT

We thank Professor Astrid Gräslund of the Department of Biophysics at Stockholm University for the permission to use the EPR spectrometer and Dr. Peter Schmidt and Mr. Torbjörn Astlind for methodological assistance.

REFERENCES

1. Brain, S. D., and Williams, T. J. (1990) *Pharmacol. Ther. 46*, 57−66.
2. Rådmark, O. (1999) in *Novel Inhibitors of Leukotrienes* (Giancarlo Folco, B. S., and Murphy, R. C., Eds.) pp 1−22, Birkhäuser, Basel.
3. Van der Heijdt, L. M., Feiters, M. C., Navaratnam, S., Nolting, H. F., Hermes, C., Veldink, G. A., and Vliegenthart, J. F. (1992) *Eur. J. Biochem. 207*, 793−802.
4. Chasteen, N. D., Grady, J. K., Skorey, K. I., Neden, K. J., Riendeau, D., and Percival, M. D. (1993) *Biochemistry 32*, 9763−9771.
5. Boyington, J. C., Gaffney, B. J., and Amzel, L. M. (1993) *Science 260*, 1482−1486.
6. Minor, W., Steczko, J., Bolin, J. T., Otwinowski, Z., and Axelrod, B. (1993) *Biochemistry 32*, 6320−6323.
7. Minor, W., Steczko, J., Stec, B., Otwinowski, Z., Bolin, J. T., Walter, R., and Axelrod, B. (1996) *Biochemistry 35*, 10687−10701.
8. Nelson, M. J., and Seitz, S. P. (1994) *Curr. Opin. Struct. Biol. 4*, 878−884.
9. Prigge, S. T., Boyington, J. C., Gaffney, B. J., and Amzel, L. M. (1996) *Proteins: Struct., Funct., Genet. 24*, 275−291.
10. Rådmark, O. (1999) in *Molecular and Cellular Basis of Inflammation* (Serhan, C. N., and P. A. W., Eds.) pp 93−108, Humana Press Inc., Totowa, NJ.
11. Gillmor, S. A., Villasenor, A., Fletterick, R., Sigal, E., and Browner, M. F. (1997) *Nat. Struct. Biol. 4*, 1003−1009.
12. Skrzypczak-Jankun, E., Amzel, L. M., Kroa, B. A., and Funk, M. O., Jr. (1997) *Proteins: Struct., Funct., Genet. 29*, 15−31.
13. Solomon, E. I., Zhou, J., Neese, F., and Pavel, E. G. (1997) *Chem. Biol. 4*, 795−808.
14. Weitzel, F., and Wendel, A. (1993) *J. Biol. Chem. 268*, 6288−6292.
15. Schewe, C., Schewe, T., and Wendel, A. (1994) *Biochem. Pharmacol. 48*, 65−74.
16. Zhang, Y. Y., Hamberg, M., Rådmark, O., and Samuelsson, B. (1994) *Anal. Biochem. 220*, 28−35.
17. Björnstedt, M., Odlander, B., Kuprin, S., Claesson, H. E., and Holmgren, A. (1996) *Biochemistry 35*, 8511−8516.
18. Walther, M., Holzhutter, H. G., Kuban, R. J., Wiesner, R., Rathmann, J., and Kühn, H. (1999) *Mol. Pharmacol. 56*, 196−203.
19. Zhang, Y. Y., Rådmark, O., and Samuelsson, B. (1992) *Proc. Natl. Acad. Sci. U.S.A. 89*, 485−489.
20. Hammarberg, T., Zhang, Y. Y., Lind, B., Rådmark, O., and Samuelsson, B. (1995) *Eur. J. Biochem. 230*, 401−407.
21. Zhang, Y. Y., Hammarberg, T., Radmark, O., Samuelsson, B., Ng, C. F., Funk, C. D., and Loscalzo, J. (2000) *Biochem. J. 351*, 697−707.
22. Bradford, M. M. (1976) *Anal. Biochem. 72*, 248−254.
23. Davydov, R., Kuprin, S., Gräslund, A., and Ehrenberg, A. (1994) *J. Am. Chem. Soc. 116*, 11120−11128.
24. Aasa, R., and Vänngård, T. (1975) *J. Magn. Reson. 19*, 308−315.
25. Sahlin, M., Gräslund, A., and Ehrenberg, A. (1986) *J. Magn. Reson. 65*, 135−137.
26. Abragam, A., and Bleany, B. (1970) *Electron Paramagnetic Resonance of Transition Ions*, Clarendon Press, Oxford.
27. Gaffney, B. J., and Silverstone, H. J. (1993) in *Biological Magnetic Resonance* (Berliner, L. J., and Reuben, J., Eds.) pp 1−57, Plenum Press, New York.
28. Scholes, C. P., Isaacson, R. A., and Feher, G. (1971) *Biochim. Biophys. Acta 244*, 206−210.
29. Slappendel, S., Veldink, G. A., Vliegenthart, J. F., Aasa, R., and Malmstrom, B. G. (1980) *Biochim. Biophys. Acta 624*, 30−39.
30. Leatherbarrow, R. J. (1992) *GraFit Version 3.0*, Eritacus Software Ltd., Staines, U.K.
31. Hagen, W. R. (1982) *Biochim. Biophys. Acta 708*, 82−98.
32. Hendrich, M. P., and Debrunner, P. G. (1989) *Biophys. J. 56*, 489−506.
33. Slappendel, S., Aasa, R., Malmström, B. G., Verhagen, J., and Veldink, G. A. (1982) *Biochim. Biophys. Acta 708*, 259−265.
34. Nelson, M. J. (1987) *J. Biol. Chem. 262*, 12137−12142.
35. Gaffney, B. J., Mavrophilipos, D. V., and Doctor, K. S. (1993) *Biophys. J. 64*, 773−783.
36. Scarrow, R. C., Trimitsis, M. G., Buck, C. P., Grove, G. N., Cowling, R. A., and Nelson, M. J. (1994) *Biochemistry 33*, 15023−15035.
37. van der Heijdt, L. M., Schilstra, M. J., Feiters, M. C., Nolting, H. F., Hermes, C., Veldink, G. A., and Vliegenthart, J. F. (1995) *Eur. J. Biochem. 231*, 186−191.
38. Pavlosky, M. A., Zhang, Y., Westre, T. E., Gan, Q. F., Pavel, E. G., Campochiaro, C., Hedman, B., Hodgson, K. O., and Solomon, E. I. (1995) *J. Am. Chem. Soc. 117*, 4316−4327.
39. Zhang, Y., Gan, Q. F., Pavel, E. G., Sigal, E., and Solomon, E. I. (1995) *J. Am. Chem. Soc. 117*, 7422−7427.

40. Holman, T. R., Zhou, J., and Solomon, E. I. (1998) *J. Am. Chem. Soc. 120*, 12564−12572.
41. Kramer, J. A., Johnson, K. R., Dunham, W. R., Sands, R. H., and Funk, M. O., Jr. (1994) *Biochemistry 33*, 15017−15022.
42. Nelson, M. J. (1988) *Biochemistry 27*, 4273−4278.
43. Hegg, E. L., and Que, L., Jr. (1997) *Eur. J. Biochem. 250*, 625−629.
44. Zhang, Y. Y., Lind, B., Rådmark, O., and Samuelsson, B. (1993) *J. Biol. Chem. 268*, 2535−2541.
45. Percival, M. D., and Ouellet, M. (1992) *Biochem. Biophys. Res. Commun. 186*, 1265−1270.
46. Feiters, M. C., Aasa, R., Malmström, B. M., Slappendel, S., Veldink, G. A., and Vliegenthart, J. F. G. (1985) *Biochim. Biophys. Acta 831*, 302−305.
47. Corey, E. J., and Nagata, R. (1987) *J. Am. Chem. Soc. 109*, 8107−8108.
48. Kuban, R. J., Wiesner, R., Rathman, J., Veldink, G., Nolting, H., Sole, V. A., and Kuhn, H. (1998) *Biochem. J. 332*, 237−242.
49. de Groot, J. J., Veldink, G. A., Vliegenthart, J. F., Boldingh, J., Wever, R., and van Gelder, B. F. (1975) *Biochim. Biophys. Acta 377*, 71−79.
50. Slappendel, S., Veldink, G. A., Vliegenthart, J. F. G., Aasa, R., and Malmström, B. G. (1983) *Biochim. Biophys. Acta 747*, 32−36.
51. Nelson, M. J., Seitz, S. P., and Cowling, R. A. (1990) *Biochemistry 29*, 6897−6903.
52. Hammarberg, T., and Rådmark, O. (1999) *Biochemistry 38*, 4441−4447.
53. Hammarberg, T., Provost, P., Persson, B., and Rådmark, O. (2000) *J. Biol. Chem. 275*, 38787−38793.
54. Kumar, S., Björnstedt, M., and Holmgren, A. (1992) *Eur. J. Biochem. 207*, 435−439.
55. Björnstedt, M., Kumar, S., and Holmgren, A. (1995) *Methods Enzymol. 252*, 209−219.
56. Holmgren, A. (2000) *Antioxid. Redox Signaling 2*, 811−820.
57. Björnstedt, M., Hamberg, M., Kumar, S., Xue, J., and Holmgren, A. (1995) *J. Biol. Chem. 270*, 11761−11764.
58. Zhong, L., Arner, E. S. J., and Holmgren, A. (2000) *Proc. Natl. Acad. Sci. U.S.A. 97*, 5854−5859.

BI001595D